A Finite Element Model for Describing the Effect of Muscle Shortening on Surface EMG

# A Finite Element Model for Describing the Effect of Muscle Shortening on Surface EMG

Luca Mesin[1], Michelle Joubert[2], Tania Hanekom[2], Roberto Merletti[1], Dario Farina[3,*]

*Abstract*—**A finite element model for the generation of single fiber action potentials in a muscle undergoing various degrees of fiber shortening is developed. The muscle is assumed fusiform with muscle fibers following a curvilinear path described by a Gaussian function Different degrees of fiber shortening are simulated by changing the parameters of the fiber path and maintaining the volume of the muscle constant. The conductivity tensor is adapted to the muscle fiber orientation. In each point of the volume conductor, the conductivity of the muscle tissue in the direction. of the fiber is larger than that in the transversal direction. Thus, the conductivity tensor changes point-by-point with fiber shortening, adapting to the fiber paths. An analytical derivation of the conductivity tensor is provided. The volume conductor is then studied with a finite element approach using the analytically derived conductivity tensor. Representative simulations of single fiber action potentials with the muscle at different degrees of shortening are presented. It is shown that the geometrical changes in the muscle, which imply changes in the conductivity tensor, determine important variations in action potential shape, thus affecting its amplitude and frequency content. The model provides a new tool for interpreting surface EMG signal features with changes in muscle geometry, as it happens during dynamic contractions.**

*Index Terms*—**electromyography, modeling, finite elements**

## I. Introduction

SURFACE EMG signal modeling has important applications in the interpretation of experimental EMG recordings [1][2][3]. Thus, in the last decades, many surface EMG models have been proposed [3], with increasing complexity and accuracy. Both numerical and analytical approaches were used to describe the electrical properties of the tissues separating the muscle fibers and the detecting electrodes (the volume conductor). The volume conductor has been considered homogeneous in many past modeling approaches [1][4], and inhomogeneous in more recent developments [5][6][7]. In the latter case, layered descriptions of the tissues, either planar [6] or cylindrical [5][7], have usually been adopted.

In most models, the volume conductor is homogeneous in the direction of propagation of the intracellular action potentials [4][5][6][7][8]. This assumption characterizes a system space-invariant in the direction of source propagation (refer to [9] for a formal definition of space-invariance). The space-invariance property significantly simplifies the analytical derivation of the surface detected potential, which is generated through the application of linear, space- and time-invariant filters to the source [6]. However, non-space-invariant systems have important relevance for interpreting EMG signal features [10].

Lack of invariance in the direction of source propagation can be due to changes in conductivity (e.g., due to localized inhomogeneities [11] or fiber pinnation [12]), or to the geometry of the volume conductor [9]. In these cases, the surface potential distributions generated by a source located at different places along the propagation path are different in shape and not simply translated versions of the same solution as it happens for space-invariant systems. Thus, analytical solutions of the problem are usually very complex. For this reason, only a few solutions for specific non-space-invariant systems have been analytically derived [11][12] while general non-space-invariant systems cannot be investigated with analytical approaches and require numerical techniques [9].

Finite element techniques have been applied in surface EMG modeling for the investigation of layered volume conductors with conductivity tensor constant in each layer [13]. However, the muscle conductivity tensor depends point-by-point on the orientation of the muscle fibers [9][12], with the conductivity in the fiber direction (which may change point-by-point in the muscle) larger than the conductivity in the direction transversal to muscle fibers. Thus, curvilinear fibers imply a complex description of the corresponding conductivity tensor. Only one previous work addressed the problem of matching the conductivity tensor of the muscle tissue to the fiber orientation in a surface EMG model [9], providing a finite element solution to the problem.

An important practical problem in the detection of surface EMG signals is the geometrical modification of the muscle due to fiber shortening, when the joint angle changes. With

1. Laboratorio di Ingegneria del Sistema Neuromuscolare (LISiN), Dipartimento di Elettronica, Politecnico di Torino, Torino, Italy
2. Department of Electrical, Electronic and Computer Engineering, University of Pretoria, Pretoria, South Africa
3. Center for Sensory-Motor Interaction (SMI), Department of Health Science and Technology Aalborg University, Aalborg, Denmark
Address for correspondence: * Dario Farina, Ph.D., Center for Sensory-Motor Interaction, Aalborg University, Fredrik Bajers Vej 7 D-3, DK-9220 Aalborg, Denmark, tel: +4596358821; fax: +4598154008, E-mail: df@hst.aau.dk

decreasing muscle length, fiber diameter increases, thus the shape of the muscle and the direction of the fibers change. This determines variations both in the geometry and conductivity tensor of the volume conductor.

In a previous study, we analyzed the effect of fiber shortening on estimated EMG variables [14]. However, we focused exclusively on the effect of end-of-fiber components on the EMG signals; these components increase as the tendon regions approach the EMG detection point, as it happens with shortening. No changes in the volume conductor geometry or conductivity tensor were included in the simulations and the conductivity tensor was constant for the entire muscle tissue. The volume conductor, described as in [6], was assumed as space-invariant in the direction of source propagation and identical in all the shortening conditions.

In this study we propose a method for simulation of surface EMG at different degrees of muscle shortening, assuming a complex volume conductor, non-space-invariant in the direction of source propagation, which changes shape and conductivity properties with shortening. The path of the current source and the muscle conductivity tensor indeed depend on the fiber orientation, which changes point-by-point and with shortening. The conductivity tensor is analytically computed; however, the complexity of the system imposes a numerical solution of the volume conductor problem, given the analytically derived conductivity tensor. Due to the complexity of the simulated condition, some simplifications were assumed. Thus, although the conductivity tensor of the muscle tissue was described in a more accurate way with respect to previous studies, source description was simplified (tripole approximation) and no additional layers (subcutaneous and skin layer, for example) were included in the model. The aim was to focus on the effects produced by the change in muscle conductivity tensor with varying fiber direction.

## II. METHODS

The bioelectrical problem of EMG simulation can be considered quasi-statical, thus the Poisson equation holds:

$$\begin{cases} -\nabla\cdot(\underline{\underline{\sigma}}\nabla\varphi) = g & \Omega \\ \underline{\underline{\sigma}}\nabla\varphi = 0 & \partial\Omega \end{cases} \quad (1)$$

where $\underline{\underline{\sigma}}$ is the conductivity tensor, $\varphi$ the electric potential, $g$ the source term (which is a current density traveling along the fiber and inducing its contraction), $\Omega$ and $\partial\Omega$ the volume conductor domain and its boundary, respectively.

In this section we will consider the volume conductor as comprised of muscle and tendon only, thus neglecting the effect of subcutaneous layers. The muscle is assumed fusiform and changes shape with shortening of its fibers.

### *2.1 Muscle geometry*

To represent a fusiform muscle, we consider fiber paths described by the following curves (Figure 1):

$$\gamma(z) = \begin{pmatrix} r(z)\cos(\theta) \\ r(z)\sin(\theta) \\ z \end{pmatrix}, \quad (2)$$

where $\theta$ identifies the radial location of the muscle fiber, and $r(z)$ is the distance of the fiber from the *z*-axis (central axis of the muscle). The most external fibers are characterized by the radius $r(z) = f(z)$, with:

$$f(z) = Re^{-\frac{z^2}{2w^2}} \quad (3)$$

where $R$ is the maximum radius of the muscle tissue (for $z = 0$) (Figure 1). The function $f(z)$ is limited to the interval $z \in [-d, d]$, such that the minimum muscle radius $R_0 = Re^{-\frac{d^2}{2w^2}}$ corresponds to the tendon thickness. The parameters $R$ and $w$ determine the geometry of the muscle. For example, the increase in $w$ increases muscle length. This description is relatively simple and allows the change in muscle geometry by varying two parameters. Moreover, it allows the definition of the fiber orientation in each point of the muscle [Eq. (2)] and, thus, the analytical calculation of the conductivity tensor in the volume conductor.

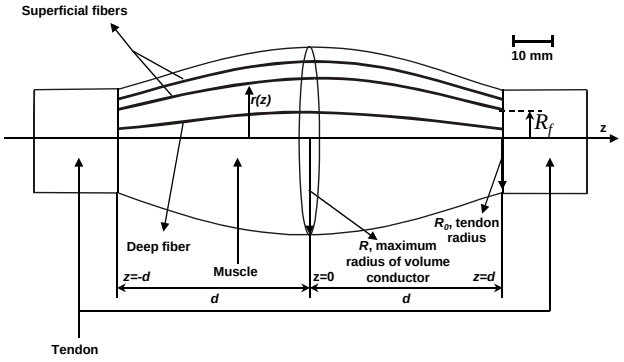


**Figure 1** A two-dimensional view of the analyzed volume conductor for a muscle length of 110 mm. The muscle geometry has in this case a tendon radius of 10 mm and a maximum radius of 18.5 mm. Note the difference in curvature of superficial and deep fibers. $R_f$ is the distance of the fiber from the *z* axis at the tendon level.

The parameters $R$ and $w$ in Eq. (3) change with shortening. We will set two constraints to determine their values: 1) the total muscle volume, and 2) the minimum radius $R_0$ (corresponding to the radius of the tendon) are constant in each shortening condition. These two constraints are not necessary for the development of the finite element model but allow a simple calculation of $R$ and $w$, given the volume of the muscle and its length (degree of shortening).

The first constrain imposes:

$$V = \int_{\Omega} \mathrm{d}V = \pi \int_{-d}^{d} r^2(z)\mathrm{d}z = wR^2\pi^{3/2}\mathrm{Erf}\left(\frac{d}{w}\right) = \text{constant} \quad (4)$$

where $\mathrm{Erf}(z) = \frac{2}{\sqrt{\pi}}\int_0^z \mathrm{e}^{-\lambda^2}\mathrm{d}\lambda$ and $d$ is half the length of the muscle.

The second constraint imposes $f(d)=R_0$, leading to the following relation:

$$d = w\sqrt{2\ln\left(\frac{R}{R_0}\right)} \quad (5)$$

Substituting Eq. (5) in Eq. (4), we obtain:

$$V = R^2\pi^{3/2}\frac{\sqrt{d^2}}{\sqrt{2\ln\left(\frac{R}{R_0}\right)}}Erf\left(\sqrt{2\ln\left(\frac{R}{R_0}\right)}\right) \quad (6)$$

which provides the value of $R$ (to be solved numerically), given the volume of the muscle, the length $2d$ of the muscle, and the radius $R_0$ of the tendon. When $R$ is determined, the parameters $w$ is obtained by Eq. (5). The parameter $w$ is the same for all fibers. The maximum distance $R_d \le R$ of each fiber from the $z$ axis is computed by assuming the ratio $R_d/R$ constant in each shortening condition. In this way, in each muscle section, the fiber density is the same for all muscle lengths.

*2.2 Conductivity tensor*

A general conductivity tensor for a muscle tissue can be expressed as [9]:

$$\underline{\underline{\sigma}} = \sigma_l \hat{v}_l \hat{v}_l + \sigma_t \hat{v}_{tn} \hat{v}_{tn} + \sigma_t \hat{v}_{tb} \hat{v}_{tb} \quad (7)$$

where the subscript $l$ stands for longitudinal and $t$ for transversal coordinate with respect to the fiber direction, and $\vec{v}_l, \vec{v}_{tn}, \vec{v}_{tb}$ are the longitudinal, normal, and binormal versors relative to the fiber orientation, respectively. Such versors are functions of the position in case of curvilinear fibers.

Poisson's equation in a Cartesian system can be obtained for a general conductivity tensor by introducing the Cartesian representation of the curvilinear differential operators (gradient and divergence), as follows:

$$\nabla\cdot\left(\underline{\underline{\sigma}}\nabla(\bullet)\right) = \begin{pmatrix}\partial_x & \partial_y & \partial_z\end{pmatrix}\left[\left(\sigma_l \hat{v}_l \hat{v}_l + \sigma_t \hat{v}_{tn} \hat{v}_{tn} + \sigma_t \hat{v}_{tb} \hat{v}_{tb}\right)\begin{pmatrix}\partial_x \\ \partial_y \\ \partial_z\end{pmatrix}\right]. \quad (8)$$

For the fusiform muscle introduced, the longitudinal, normal, and binormal vectors become:

$$\vec{v}_l = \begin{pmatrix}\dot{r}\cos(\theta) \\ \dot{r}\sin(\theta) \\ 1\end{pmatrix} = \begin{pmatrix}-\frac{zx}{w^2} \\ -\frac{zy}{w^2} \\ 1\end{pmatrix};\quad \vec{v}_{tn} = \begin{pmatrix}\cos(\theta) \\ \sin(\theta) \\ -\dot{r}\end{pmatrix} = \begin{pmatrix}\frac{x}{\sqrt{x^2+y^2}} \\ \frac{y}{\sqrt{x^2+y^2}} \\ \frac{z}{w^2}\sqrt{x^2+y^2}\end{pmatrix};\quad \vec{v}_{tb} = \begin{pmatrix}-\sin(\theta) \\ \cos(\theta) \\ 0\end{pmatrix} = \begin{pmatrix}-\frac{y}{\sqrt{x^2+y^2}} \\ \frac{x}{\sqrt{x^2+y^2}} \\ 0\end{pmatrix}. \quad (9)$$

where the point over a symbol indicates the first derivative with respect to $z$. Using their normalized versions in the general expression (8), calculations (omitted) yield the following expression of the conductivity tensor in a Cartesian system for the fusiform muscle defined by the fiber orientation in Eq. (2):

$$\underline{\underline{\sigma}} = \frac{1}{w^4 + z^2\left(x^2+y^2\right)}\begin{bmatrix} x^2z^2\sigma_l + \left(w^4+y^2z^2\right)\sigma_t & xyz^2\left(\sigma_l-\sigma_t\right) & -w^2xz\left(\sigma_l-\sigma_t\right) \\ xyz^2\left(\sigma_l-\sigma_t\right) & y^2z^2\sigma_l + \left(w^4+x^2z^2\right)\sigma_t & -yzw^2\left(\sigma_l-\sigma_t\right) \\ -w^2xz\left(\sigma_l-\sigma_t\right) & -yzw^2\left(\sigma_l-\sigma_t\right) & w^4\sigma_l + z^2\left(x^2+y^2\right)\sigma_t \end{bmatrix} \quad (10)$$

This is the tensor to be used in a finite element model for describing the conductivity properties of the muscle tissue point-by-point under different degrees of shortening.

*2.3 Source description*

The modeling of the generation, propagation, and extinction of the intra-cellular action potential has been extensively addressed in past work [4][15][16][17]. The general assumption is that the integral of the current density over the muscle fiber length is zero in each instant of time. For volume conductors which are not space-invariant in the direction of propagation, as that studied in this work, the response of the system to an impulsive current depends on the position of the current (thus, it is not an impulse response in the sense of linear and space-invariant spatial filtering). The source function should be sampled and viewed as a multi-pole. The tripole approximation of the transmembrane current density [18] was used in this study. Generation and extinction of the intracellular action potentials at the end-plate and tendons were included as described by Merletti et al. [1]. The path of propagation of the transmembrane current was defined by the curve $\gamma$ in Eq. (2), which also determined the conductivity tensor. The arch length of $\gamma$ was used as the coordinate to locate the tripole source within the muscle and to describe its propagation [9].

*2.4 Numerical implementation*

The numerical approach applied was based on finite elements and implemented by the software package FEMLAB (version 3.0a). The boundary conditions for the muscle were homogeneous Neumann conditions [19]. A Neumann boundary (also referred as natural boundary) condition specifies the value of the normal flux across the boundary. By the image theorem, Neumann boundary conditions lead to periodicity [19]. A sub-domain representing the tendon ending was added to the muscle geometry (Figure 1) in order to reduce aliasing.

The periodicity given by the Neumann boundary conditions can be used to reduce computational time. From image theory, cutting the muscle geometry in two halves, it is possible to study two propagating tripoles by simulating only one (the second is an image of the first). Thus, in order to save computational time, only half of the original volume conductor can be described (Figure 2), imposing the Neumann boundary conditions at $z = 0$ which account for the second half of the volume conductor (image of the first half). This approach is valid only for symmetric muscle fibers, with the end-plate in the middle of the volume conductor. If the muscle fibers are

asymmetric, the entire volume conductor and the two tripoles should be studied.

The tendon ending was considered isotropic (conductivity 0.3 S/m), while the muscle tissue was electrically described by the conductivity tensor in Eq. (10) (in-homogeneous and anisotropic), with $\sigma_l$ and $\sigma_t$ 0.5 S/m and 0.1 S/m, respectively.

To calculate the surface potential, the source was moved step-wise along the fiber path described by Eq. (2). Given the conduction velocity $v$ of the intracellular action potential and the sampling rate $f_s$ in time domain, $v/f_s$ is the step by which the source is moved between two sampling instants. For each sampling instant, the potential distribution over the entire muscle surface was computed by meshing the volume conductor using tetrahedral elements (Figure 2). The elements surrounding the source were smaller than the others (maximum diameter of these elements 0.1 mm), to improve accuracy. The potential was calculated at the nodes located at the vertices of the tetrahedral elements [13]. Point electrodes were simulated. To obtain the potential at the muscle surface corresponding to the exact location of the electrode, the potential values at the four nodes nearest to the detection point were interpolated. This was done by calculating the distance of each node from the electrode, and summing the potentials at the nodes by a convex linear combination (i.e., with unitary sum of the weights) with weights proportional to the inverse of the distances (which is the rate of decrease of the free-space potential in the three-dimensional space, neglecting the effect of anisotropy within the specific element).

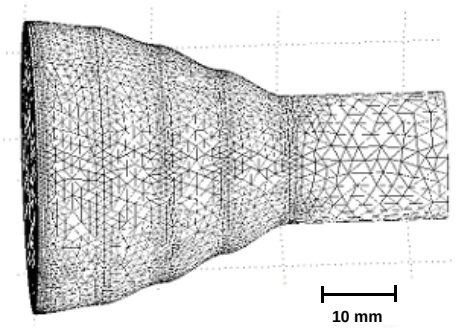


**Figure 2** A three-dimensional view of the volume conductor described by finite elements. Because of image theory, the muscle geometry has been halved (see text for details). The volume conductor (muscle and tendon) is meshed into approximately 100000 tetrahedral elements.

## III. Results

The model described was used to generate single fiber action potentials and interference surface EMG signals on the muscle surface at five stages of shortening (Figure 3). The muscle modeled was the biceps brachii. The parameters related to the five geometries are reported in Table 1 and correspond to anatomical data provided in the literature [20]. The specific shape of the volume conductor is not a constraint for the model.

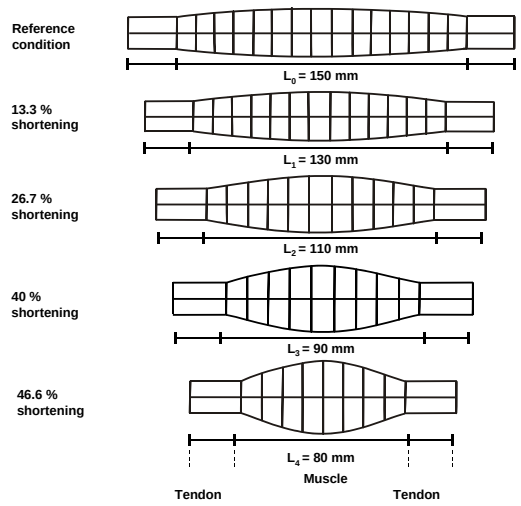


**Figure 3** A two-dimensional view of the five volume conductor shapes investigated, which correspond to different degrees of shortening. Note that only the muscle geometry shortens while the tendon regions remain of the same length and diameter in all conditions.

**Table 1** Simulation parameters for the five stages of shortening. Stage 1 is considered as the reference condition. The percentage of shortening is computed for the other stages with respect to Stage 1.

| Model Parameter | Stage 1 | Stage 2 | Stage 3 | Stage 4 | Stage 5 |
|---|---|---|---|---|---|
| $R_0$ | 10 mm | 10 mm | 10 mm | 10 mm | 10 mm |
| $R$ | 15 mm | 16.5 mm | 18.5 mm | 21 mm | 23 mm |
| $L=2d$ | 150 mm | 130 mm | 110 mm | 90 mm | 80 mm |
| Shortening (%) | 0 | 13.3 | 26.7 | 40 | 46.6 |
| $w$ | 83.29 | 64.95 | 49.58 | 36.94 | 30.99 |
| $V$ | 83.2 $cm^3$ | 83 $cm^3$ | 83.4 $cm^3$ | 83 $cm^3$ | 85.1 $cm^3$ |
| $CV$ | 4 m/s | 4 m/s | 4 m/s | 4 m/s | 4 m/s |

The recording electrode system was placed over the surface at the medium point between the fiber end-plate and the tendon ending in all conditions. Relative shift of the muscle fibers with respect to the skin surface may occur when the joint angle changes [21]. This effect was, however, not considered in the representative simulations shown in the following, to focus only on the effects of muscle shortening. Monopolar, single differential, and double differential recording systems were simulated. For single and double differential detection, the interelectrode distance was 5 mm.

Figure 4 shows examples of monopolar single fiber action potentials detected over the muscle surface with point electrodes at the five shortening stages. The action potentials simulated with the homogeneous conductivity tensor are compared with those obtained with the conductivity tensor described in Eq. (10). Action potential shape changes with shortening due to the modification in muscle geometry and in the orientation of the muscle fibers. The homogeneous and inhomogeneous descriptions of the conductivity tensors lead to a different effect on the generated action potentials.

Figures 5 and 6 show the average rectified value (ARV) and mean power spectral frequency (MNF) estimated from the simulated single fiber surface potentials at the five stages of shortening for fibers at different depths. ARV and MNF are influenced by muscle shortening, mainly due to the change in the distance between the sources and the detection electrodes with shortening. Figure 7 reports a simulation of the interference surface EMG signal at the different shortening conditions. In this case, all the physiological parameters are constant and only the geometry is changed.

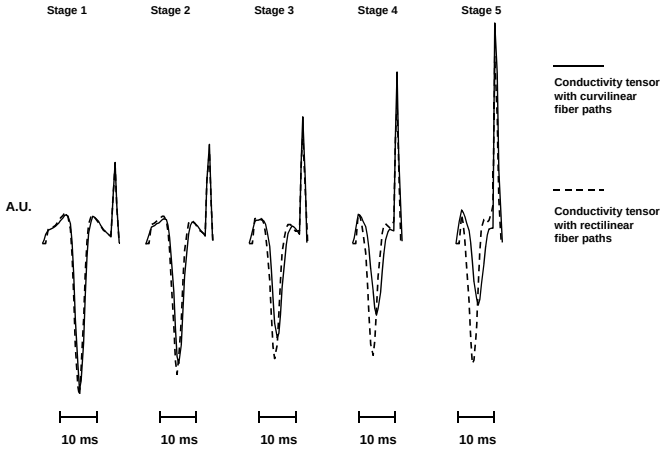


**Figure 4** Examples of surface single fiber monopolar action potentials generated at five stages of shortening. The distance of the fiber from the *z* axis is $R_f$ = 6.25 mm at the tendon level. The five stages of shortening refer to the volume conductors described in Figure 3. The conductivity tensor is described as in Eq. (10) (solid lines) and as homogeneous (dashed lines). In both cases and for all shortening conditions, the end-plate is located in the middle of the fiber, the electrodes are placed in the middle between end-plate and tendon, and the fiber is directly under the electrodes [$\theta = 0$ in Eq. (2)]. A.U. stands for arbitrary units.

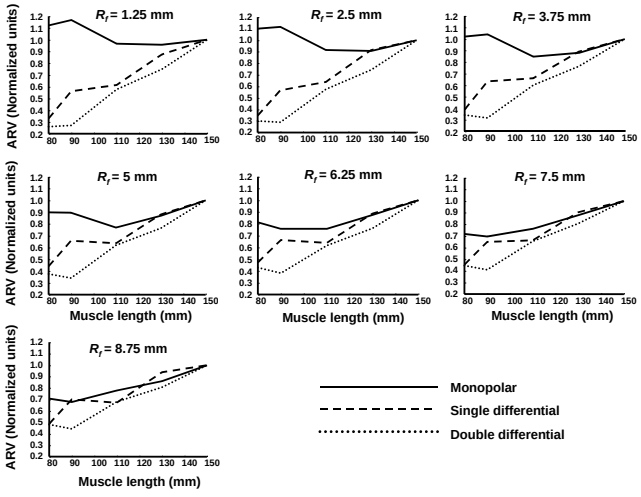


**Figure 5** ARV computed from simulated muscle fiber action potentials for the five muscle lengths described in Figure 3. Monopolar, single differential, and double differential detection systems are compared. In all conditions, the detection electrodes are located at 10° from the simulated muscle fiber in the angular direction and in the middle between the end-plate and tendon in the longitudinal direction. The end-plate is in the middle of the fiber in all cases. Interelectrode distance for the bipolar and double differential recordings is 5 mm. ARV is normalized with respect to the values at the reference muscle condition (stage 1 in Figure 3). The simulated fiber is located within the muscle at seven depths, corresponding, at the tendon level, to a distance $R_f$ from the *z* axis (see Figure 1) in the range 1.25-8.75 mm (1.25 mm increments). The smaller the distance, the deeper the fiber.

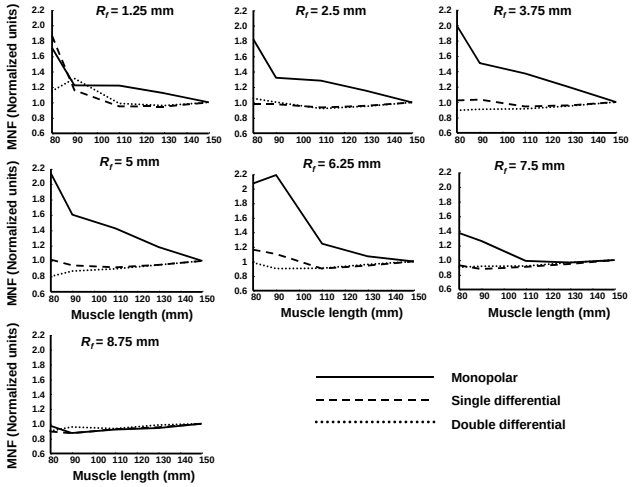


**Figure 6** MNF computed from simulated muscle fiber action potentials for the five muscle lengths defined in Figure 3. The simulations are in the same conditions as in Figure 5. MNF values are normalized with respect to the values in the reference condition.

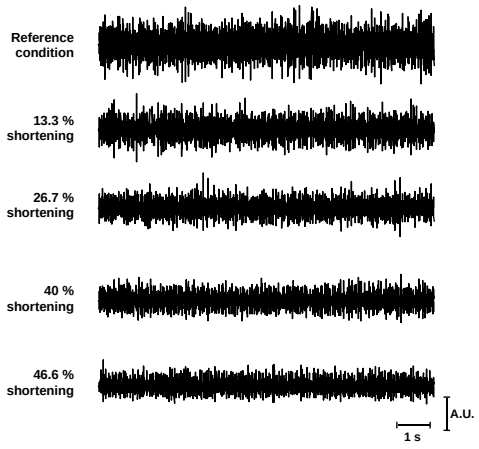


**Figure 7** Interference surface EMG signal generated by simulating the activity of 120 motor units, randomly located within the part of the muscle with distance smaller than 10 mm from the detection electrodes. The motor unit action potentials were generated from the five volume conductors depicted in Figure 3, which represent five degrees of muscle shortening. The same fibers were simulated in each shortening condition. The discharge rates of the active motor units were computed as suggested by Fuglevand et al. [28], with excitation level corresponding to 50% of the maximum. The number of fibers

in each motor unit varied randomly in the range 50-800. For each degree of shortening, the solution for the surface potential at each angular position was obtained from a set of 8 depths, to reduce computational time. The values of the potential distribution for the other depths were obtained by interpolation. Mean motor unit conduction velocity was 4 m/s and the standard deviation of conduction velocity distribution was 0.3 m/s. The motor unit discharge frequencies and conduction velocities were the same in the five conditions (no physiological changes in the five conditions). The detection system was bipolar with 5 mm interelectrode distance. A.U. stands for arbitrary units.

## IV. Discussion and Conclusions

In this study we proposed the modeling of a fusiform muscle by a finite element approach. We applied a precise analytical calculation of the conductivity tensor in each point of the muscle tissue, considering that the conductivity of the muscle depends point-by-point on the direction of its fibers. Given the analytical expression of the curve defining the fiber orientation in the muscle tissue, the conductivity tensor can be analytically computed [Eq. (10)]. Modeling the conductivity tensor of the muscle tissue has been largely neglected in the literature on EMG simulation even in the case of sources traveling along a general curvilinear path [1][22][23]. Recently, we have addressed this issue for bi-pinnate muscles [9][12]. The non-constant conductivity tensor introduces an inhomogeneity in the volume conductor in the direction of source propagation, in addition to the inhomogeneity due to geometry.

With respect to isometric contractions, dynamic exercises are more common in daily-life activities and are of greater interest in fields such as sport, space, occupational medicine, and rehabilitation. Although in recent years there have been important efforts in the development of analysis tools for surface EMG signals recorded in dynamic tasks, there are still many open issues in the interpretation of surface EMG in these conditions. Due to the lack of surface EMG models which simulate changes in muscle geometry, indications on the limitations of the surface EMG technique when applied in dynamic contractions are missing. For this reason, constrained conditions, such as cycling exercises, were usually considered (e.g., [24]).

When muscle fibers shorten, their diameters increase and, as a consequence, muscle geometry changes. A fiber at a specific depth within the muscle in resting conditions may be at a larger depth when the overlaying fibers increase their diameter, as has been simulated in this work. Thus, in addition to changes in the relative location of the tendons and end-plates with respect to the recording electrodes [14], the surface detected potentials are affected by variations in 1) the conductivity properties of the muscle tissue and 2) the relative electrode-source distance. These changes are reflected in the amplitude and frequency variables extracted from surface EMG signals (Figures 5 and 6). The simulation of only a geometrical change in the volume conductor leads to a different effect with respect to the inclusion of variations in both geometry and conductivity tensor (Figure 4).

The representative simulations shown provide an indication of the effect of changes in the conductivity tensor accompanying muscle shortening on the properties of the surface detected potentials. These effects are complex to predict without a numerical model since shortening implies a number of changes in the system. There are two main signal components which contribute to the surface EMG potentials, the propagating and the non-propagating ones. The propagating component is generated during the traveling of the intracellular action potential along the fiber, while the non-propagating component originates when the intracellular action potential generates and extinguishes at the end-plate and tendons, respectively. Since the fiber changes position within the muscle and the end-plate and tendon endings get closer to each other and to the detection electrodes with fiber shortening, the sources of the two main signal components change their relative distance with respect to the detection electrodes with decreasing fiber length. Moreover, the electrical properties and geometry of the tissue separating sources and electrodes also change. This complex set of electrical and geometrical modifications affects the surface-detected action potential in a way that is dependent on the specific detection system.

As a consequence of muscle shortening, ARV of single fiber action potentials may be reduced up to approximately one third of its initial value when muscle length is reduced to approximately 50% and the signals are detected with a bipolar system (Figure 5). The effect is smaller for superficial than for deeper fibers since the distance of superficial fibers from the electrodes changes less with shortening than that of the deep fibers. Since most of the surface EMG signal power is due to the activity of superficial fibers, the changes in ARV of the interference EMG signal are more limited than those obtained for deep single fibers but still significant in practical applications. The effect on ARV depends on the detection system. While single and double differential systems lead to similar sensitivities to muscle shortening, monopolar recordings are much less sensitive to it. This is due to the relative weight of non-propagating potentials, which is larger for monopolar than for differential recordings. As the muscle shortens, the fibers increase their distance from the detection point but the end-plate and tendon endings approach the electrodes, thus the propagating component decreases and the non-propagating one increases in amplitude, counteracting each other. This effect is less evident for single and double differential systems since these systems largely reduce the non-propagating components (DC in the spatial domain).

As for ARV, the effect of shortening on MNF depends on the depth of the fiber and on the detection system (Figure 6). The action potentials generated by superficial fibers are less affected by shortening than those from deep fibers, as discussed for ARV. In general, MNF tends to increase with shortening for the monopolar recording while this is less evident for the other two detection systems. The increase in MNF reveals the well-known larger frequency bandwidth of the non-propagating signal components with respect to the propagating parts of the signal [25][26]. As muscle shortens, the relative weight of end-plate and end-of-fiber components

increases, especially for the monopolar recording, as discussed above. However, the effect on the spectral content of the surface signal is also significantly altered by the change in the geometry and conductivity tensor of the system, which may lead to an opposite trend of MNF with shortening, i.e., to a decrease, which is observed for superficial fibers.

The comparison of these results with those obtained in experimental conditions in previous studies is difficult since in experimental studies the activation strategies of the motor units at different joint angles can not be controlled. Rainoldi et al. [21] reported significant changes in surface EMG amplitude with muscle shortening depending on the location of the recording electrodes. These changes were probably due to the concomitant effect of the relative shift of the skin with respect to the muscle (not simulated in the results shown in this study) and of muscle shortening. Similar considerations hold for frequency variables [27].

Although no movement was included in the model (i.e., the volume conductor geometry did not change during the propagation of each intra-cellular action potential), the model proposed can be used to simulate surface EMG signals detected during a dynamic task, assuming that the changes in muscle geometry occur in a time interval much longer than that needed for the propagation of the action potential along the muscle fiber. Since the interval of time between generation and extinction of an action potential is 20-30 ms, this constraint is not critical. To simulate signals during dynamic contractions, the muscle length (i.e., the shape of the volume conductor) can be specified for each activation of a specific muscle fiber. The length will be the same during the interval of time needed for the complete generation of the surface action potential but may change for each discharge of each muscle fiber. This provides the means for assessing the effect of geometrical factors on the features of surface EMG signals detected during movement, an issue on which many past works have focused with simpler models (e.g., [14][21][24][27]). The representative results on single fiber action potentials presented in this study (Figures 4, 5, and 6) underline that amplitude and spectral content of the signal may significantly change due to changes in muscle length, independently on the intensity of muscle activation or on the population of active motor units.

The specific muscle shape and the way to simulate shortening are not a constraint of the proposed model. By deriving the Cartesian representation of the conductivity tensor starting from the analytical description of the fiber orientation, the concepts proposed in this study can be applied to generic muscle shapes and fiber orientations.

### *4.1 Limitations*

The proposed model provides a more accurate description of the volume conductor with respect to past approaches when the muscle shortens. In particular, the variation in conductivity tensor due to the variation in geometry is accounted in the present approach. Nevertheless, there are simplifications in other parts of the surface EMG generation which are more restrictive than in other models. For example, the source is described as a current tripole while previous non-space-invariant models had no limitations in the shape of the intracellular action potential (e.g., [4][6]). The assumption that the tendon radius does not change with shortening also underlines that the fiber diameter should change in a different way along the fiber path, which should result in a non-constant conduction velocity during propagation. However, this effect was not simulated. Moreover, only the muscle tissue has been included in the results shown while previous models have indicated the importance of subcutaneous layers in the properties of the surface detected action potentials [16].

More complex descriptions of the sources and inclusion of additional layers are possible by increasing the complexity and computation time of the model. However, clearly any model constitutes a simplification of the real condition. Thus, the use of a specific model should be decided on the basis of the question to be addressed, maintaining the complexity at the minimum for the question at hand. The present model has been designed for investigating the influence of geometrical modifications in the muscle on the recorded surface EMG signal. To describe these effects, a finite element approach has been applied, which is computationally less efficient than analytical methods [4]. It has been shown that the accurate description of the conductivity tensor is relevant for the generation of the surface action potentials (Figure 4). While previous approaches considered only the relative shift of end-plates and tendon endings with fiber shortening [14], this study indicates that there are additional factors that affect the signal properties when the muscle shortens. In particular, it is shown that not only the non-propagating components but also the propagating ones changes with shortening.

### *4.2 Conclusion*

This study proposes an approach for precisely simulating surface EMG signals as generated by a muscle at different lengths. The model is innovative with respect to previous approaches since it provides, for the first time, the description of the muscle conductivity tensor according to the orientation of the muscle fibers during shortening. This model constitutes an important tool for interpreting surface EMG signal features in dynamic tasks.

## REFERENCES

[1] R. Merletti, L. Lo Conte, E. Avignone, P. Guglielminotti, “Modeling of surface EMG signals. Part I: model and implementation,” *IEEE Trans. on Biomed. Eng.*, vol. 46, pp. 810-820, 1999

[2] R. Merletti, S.H. Roy, E. Kupa, S. Roatta, A. Granata, “Modeling of surface myoelectric signals--Part II: Model-based signal interpretation,” *IEEE Trans. Biomed. Eng.*, vol. 46, pp. 821-829, 1999

[3] D.F. Stegeman, J.H. Blok, H.J. Hermens, K. Roeleveld, “Surface EMG models: properties and applications,” *Journ. Electromyogr. Kinesiol.*, vol. 10, pp. 313-26, 2000

[4] G.V. Dimitrov, N.A. Dimitrova, “Precise and fast calculation of the motor unit potentials detected by a point and rectangular plate electrode,” *Med. Eng. Phys.*, vol. 20, pp. 374-381, 1998

[5] J.H. Blok, D.F. Stegeman, A. van Oosterom, "Three-layer volume conductor model and software package for applications in surface electromyography," *Ann. Biomed. Eng.*, vol. 30, pp. 566-577, 2002
[6] D. Farina, R. Merletti, "A novel approach for precise simulation of the EMG signal detected by surface electrodes," *IEEE Trans. Biomed. Eng.*, vol. 48, pp. 637-646, 2001
[7] D. Farina, L. Mesin, S. Martina, R. Merletti, "A surface EMG generation model with multi-layer cylindrical description of the volume conductor," *IEEE Trans. Biomed. Eng.*, vol. 51, pp. 415-426, 2004
[8] J. Duchene, J.Y. Hogrel, "A model of EMG generation," *IEEE Trans. Biomed. Eng.*, vol. 47, pp. 192-201, 2000
[9] D. Farina, L. Mesin, S. Martina, "Advances in surface electromyography signal simulation with analytical and numerical descriptions of the volume conductor," *Med. Biol. Eng. Comput.*, vol. 42, pp. 467-76, 2004
[10] D. Farina, L. Mesin, "Sensitivity of surface EMG-based conduction velocity estimates to local tissue in-homogeneities – influence of the number of channels and inter-channel distance," *J. Neurosci. Meth.*, in press
[11] L. Mesin, D. Farina, "A model for surface EMG generation in volume conductors with spherical in-homogeneities," IEEE Trans. Biomed. Eng., submitted
[12] L. Mesin, D. Farina, "Simulation of surface EMG signals generated by muscle tissues with in-homogeneity due to fiber pinnation," *IEEE Trans. Biomed. Eng.*, vol. 51, pp. 1521-1529, 2004
[13] M.M. Lowery, N.S. Stoykov, A. Taflove, T.A. Kuiken, "A multiple-layer finite-element model of the surface EMG signal," *IEEE Trans. Biomed. Eng.*, vol. 49, pp. 446-54, 2002
[14] E. Schulte, D. Farina, R. Merletti, G. Rau, C. Disselhorst-Klug, "Influence of muscle fiber shortening on estimates of conduction velocity and spectral frequencies from surface electromyographic signals," *Med. Biol. Eng. Comput.*, vol. 42, pp. 477–486, 2004
[15] N.A. Dimitrova, "Model of the extracellular potential field of a single striated muscle fiber," *Electromyogr. Clin. Neurophysiol.*, vol. 14, pp. 53-66, 1974
[16] T.H. Gootzen, D.F. Stegeman, A. Van Oosterom, "Finite limb dimensions and finite muscle length in a model for the generation of electromyographic signals," *Electroenc. Clin. Neurophysiol.*, vol. 81, pp. 152-162, 1991
[17] P. Griep, F. Gielen, K. Boon, L. Hoogstraten, C. Pool, W. Wallinga de Jonge, "Calculation and registration of the same motor unit action potential," *Electroencephalogr. Clin. Neurophysiol.*, vol. 53, pp. 388-404, 1982
[18] K. McGill, A. Huynh, "A model of the surface recorded motor unit action potential," *Proc. 10th Ann. Int. IEEE Conf. Eng. Med. Biol.*, pp. 1697-1699, 1988
[19] P.P. Silvester, R.L. Ferrari *"Finite elements for electrical engineers,"* 3 rd edition ed Cambridge university press, Cambridge, 1983
[20] B.A. Garner, M.G. Pandy, "Estimation of musculotendon properties in the human upper limb," *Ann. Biomed. Eng.*, vol. 31, pp. 207-20, 2003
[21] A. Rainoldi, M. Nazzaro, R. Merletti, D. Farina, I. Caruso, S. Gaudenti, "Geometrical factors in surface EMG of the vastus medialis and lateralis muscles," *J. Electromyogr. Kinesiol.*, vol. 10, pp. 327-36, 2000
[22] N.A. Dimitrova, A.G. Dimitrov, G.V. Dimitrov, "Calculation of extracellular potentials produced by an inclined muscle fibre at a rectangular plate electrode," *Med. Eng. Phys.*, vol. 21, pp. 583-8, 1999
[23] S. Xiao, K.C. Mc Gill, V.R. Hentz, "Action potentials of curved nerves in finite limbs," *IEEE Trans. Biomed. Eng.*, vol. 42, pp. 599-607, 1995
[24] D.T. MacIsaac, P.A. Parker, R.N. Scott, K.B. Englehart, C. Duffley, "Influences of dynamic factors on myoelectric parameters," *IEEE Eng. Med. Biol. Mag.*, vol. 20, pp. 82-9, 2001
[25] N.A. Dimitrova, G.V. Dimitrov, O.A. Nikitin, "Neither high-pass filtering nor mathematical differentiation of the EMG signals can considerably reduce cross-talk", *J. Electromyogr. Kinesiol.*, vol. 12, pp. 235-246, 2002
[26] D. Farina, R. Merletti, B. Indino, M. Nazzaro, and M. Pozzo, "Cross-talk between knee extensor muscles. Experimental and model results," *Muscle Nerve*, vol. 26, pp. 681-95, 2002
[27] D. Farina, R. Merletti, M. Nazzaro, I. Caruso, "Effect of joint angle on EMG variables in leg and thigh muscles," *IEEE Eng. Med. Biol. Mag.*, vol. 20, pp. 62-71, 2001
[28] A.J. Fuglevand, D.A. Winter, A.E. Patla, "Models of recruitment and rate coding organization in motor-unit pools", *J. Neurophysiol.*, vol. 70, pp. 2470-88, 1993

**Luca Mesin** graduated in electronics engineering in December 1999 from Politecnico di Torino, Torino, Italy, he received the Ph.D. in Applied Mathematics in 2003, from the same university. Since March 2003, he is a Fellow of the Laboratory for Neuromuscular System Engineering in Torino. He was involved in research activities in the fields of Kinetic theory and Deformable Porous Media theory, with applications to Biomathematics and Composite Materials. Now, his main research interests concern signal processing of biomedical signals and modeling of biological systems.